Real-time Indication of Acoustic Window for Phased-Array Transducers in Ultrasound Imaging

Lasse Løvstakken* and Fredrik Orderud†, and Hans Torp*
*Department of Circulation and Medical Imaging
†Department of Computer and Information Science
Norwegian University of Science and Technology, Trondheim, Norway

***Abstract*—In ultrasound imaging, the transducer aperture may be partly obstructed due to a lack of acoustic contact with the patient skin, or from objects close to the transducer surface such as a patient's ribs. For phased-array operation, such a reduction of imaging aperture results in a gradual degradation in image quality in terms of a reduced lateral resolution and a loss in penetration. This loss in image quality is not always obvious and may result in that inferior images are used in further diagnosis.**

A method for real-time feedback of the acoustic contact along phased-array transducers has been developed. The method is based on the Fraunhofer approximation, which implies that the lateral power spectrum close to focus is bandlimited by the convolution of the transmit and receive aperture functions. By estimating and visualizing the lateral power spectrum, an image of the acoustic contact can be produced.

Using data from a tissue-mimicking phantom, we show that the lateral power spectrum closely corresponds to the effective aperture used for 0-100 % acoustic contact. The method was further evaluated for *in vivo* cardiac imaging, where we show that the obstruction of sound caused by the human sternum similarly can be observed in the lateral spectrum, and therefore indicate that a more suitable probe position should be sought.

I. Introduction

In ultrasound imaging, the transducer aperture used in image formation may be partly obstructed due to a lack of acoustic contact with the patient skin, or by dense objects just beneath the skin surface. For linear scan operation, in which a smaller part of the transducer aperture is swept across the array, no image is produced for the obstructed region which can easily be identified. For phased-array operation however, all aperture elements typically contribute in the image formation through beam focusing and steering. When parts of the imaging aperture is obstructed, a complete image will still be shown, but the reduction in imaging aperture will lead to a degradation of image quality. In particular, the lateral image resolution is reduced and a loss in penetration will occur.

The reduction of the effective imaging aperture may arise in different contexts. A poor skin contact may be caused by the use of an insufficient amount of contact gel, and can especially be a problem when the probe surface is not parallel to the skin surface. Even if the acoustic contact with the skin is sufficient, objects such as a patient rib's may limit the image formation of deeper structures. Both these cases may for instance occur in cardiac imaging due to the narrow acoustic window between the patient's ribs.

While performing an ultrasound investigation, the experienced examiner may recognize the occurrence of, for example, an inferior lateral image resolution, and try adjust the probe position accordingly. However, it is not always obvious that the image quality has been compromised. For less experienced users, identifying these problems and performing adjustments can be challenge, and may result in that images with an inferior quality are used as the basis for diagnosis.

In this work, a method for the visualization of the effective aperture of phased-array transducers is described. The method operates in real-time during acquisition, and can indicate if a contiguous part of an aperture do not contribute in the image formation. We believe the method can be help ensure that a good image quality is obtained in contexts where the acoustic contact or window is likely to be reduced.

The method is based on the k-space formulation of the ultrasound imaging system, which has proven useful for investigating imaging system performance, and which previously has been used to describe phenomena such as anisotropic scattering, speckle reduction techniques, and the correlation properties of moving objects [1], [2], [3]. It follows from the Fraunhofer approximation that the lateral bandwidth of the imaging system in the far field or near the focus is limited by the convolution of the transmit and receive aperture functions [4]. If parts of the imaging aperture is not contributing to the image formation, the lateral spectrum will be altered accordingly. Therefore, by estimating and visualizing the lateral power spectrum from the received data around the transmit focus, a map of the effective aperture used during imaging can be produced. In this work, we limit our aim to estimating and visualizing the effective aperture resulting from a contiguous obstruction of one or both ends of a phased-array transducer. The lateral bandwidth will then be reduced, and its center location relative to zero frequency in the lateral spectrum is shifted according to the remaining active aperture.

II. Theory

A. The Fraunhofer approximation

The Fraunhofer approximation, when applied to pulse-echo ultrasound imaging, implies that the two-way beam profile in the far field or focal plane of a focused transducer is bandlimited in k-space by the convolution of the apodization functions on transmit and receive [4], [3]. This intuitive relation is often used to characterize the approximate performance of ultrasound imaging systems. When neglecting phase terms

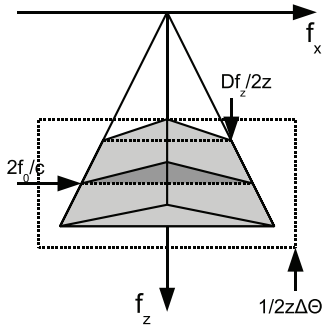

Fig. 1. An illustration of the k-space representation of an ultrasound imaging point spread function (PSF) in focus, assuming rectangular and equal transmit and receive apertures. As can be seen, the resulting lateral spectrum is then triangular shaped, centered around zero frequency. An example of the Nyquist limits for sampling the given k-space representation is given by the dotted box.

and amplitude scaling, a *simplified k-space* representation of the lateral spectrum can be expressed as [3]:

$$P_{TR}(f_x, f_z) = A_T(-2z_f f_x/f_z) *_{f_x} A_R(-2z_f f_x/f_z), \quad (1)$$

where $P_{TR}(f_x, f_z)$ is the two-way pressure field evaluated at spatial frequencies f_x and $f_z = 2f_0/c$, A_T and A_R are the apodized transmit and receive aperture functions evaluated at spatial frequencies $-2z_f f_x/f_z$, and where z_f is a depth coordinate in the focal region or far field. The Fraunhofer approximation is valid at a single frequency, but can assuming linear propagation be extended to pulsed wave excitations through superposition.

For the case of continuous transmit and receive apertures of equal length D with rectangular apodization, this effectively bandlimits the lateral spectrum towards a triangular shape in the interval $f_x \in [-D/\lambda z_f,\ +D/\lambda z_f]$. The frequency content in the axial direction is limited by the bandwidth of the transducer elements. The resulting k-space representation of an ultrasound imaging system is illustrated in Fig. 1. As can be observed, the lateral bandwidth is a function of the emitted frequency and the transmit and receive F-number.

B. The effective aperture map

Considering the relation between lateral bandwidth and imaging aperture, a map of the effective two-way imaging aperture can be estimated by lateral spectral analysis of the received signal in the region of focus. If only a part of a total aperture contributes in the imaging process due to a lack of contact or due to obstructions, the lateral spectrum will be altered accordingly. This principle is shown in Fig. 2 for two cases with 100 % and 50 % effective apertures. The resulting two-way point-spread functions were simulated using the Field II simulation software [5] (see figure caption for simulation setup). As can be seen in the bottom row plots, the lateral bandwidth is scaled and shifted in frequency due to a reduction in effective aperture.

C. Image sampling requirements

The azimuthal distance between neighboring beams is given by $z_f \Delta\theta$, where $\Delta\theta$ is the inter-beam angle in phased-array operation. The highest lateral k-space frequency before aliasing occurs then becomes:

$$f_{x,Ray} = \pm \frac{1}{2z_f \Delta\theta}. \quad (2)$$

In order to avoid aliasing artifacts when estimating the lateral spectrum, the beam density should at least satisfy the Rayleigh criterion of $f_{\#}\lambda$, where $f_{\#}$ is the two-way f-number.

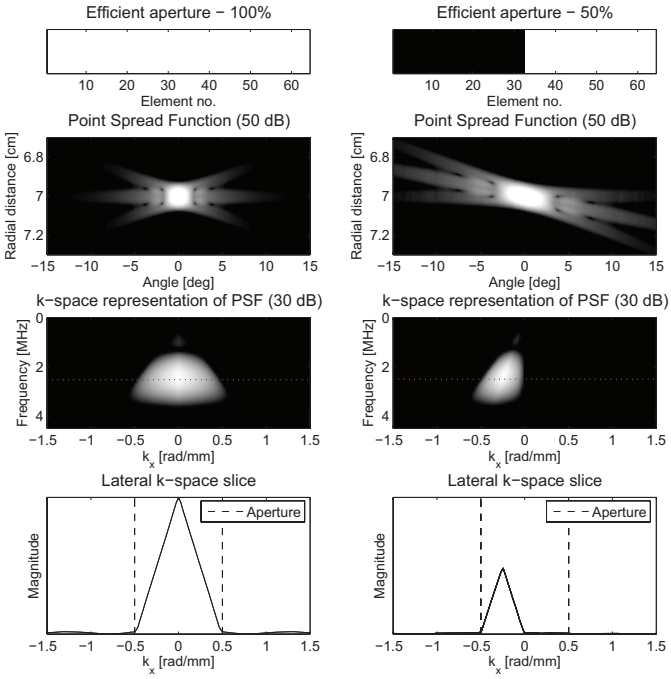

Fig. 2. An illustration of the point spread function (upper row, 50 dB dynamic range) and its k-space representation (middle row, 30 dB dynamic range) for a point scatterer in focus, when using an effective imaging aperture of 100 % (left column) and 50 % (right column) respectively. The images were simulated using Field II [5] for a 64 element 1-D phased-array transducer with equal rectangular apodization on tx/rx, operating at a center frequency $f_0 = 2.5$ MHz and with an F-number of 3.5. In the bottom row, the lateral spectrum slice at f_0 (dotted red line) is shown, illustrating the resulting 50 % bandwidth reduction for the second aperture.

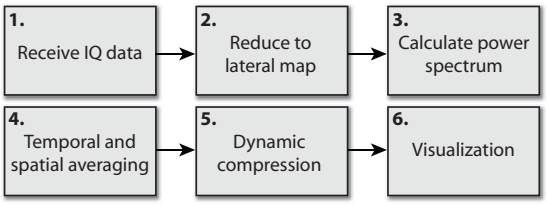

Fig. 3. A block diagram illustrating the processing chain for generating the map of acoustic contact along a phased-array transducer aperture.

III. Methods

A block diagram of the method from data acquisition to display is shown in Fig. 3. Referring to the block diagram, each processing step will be described in more detail in the following sections.

1) Receive IQ data: Processing initiates after the acquisition of a frame of complex demodulated (*IQ*) data. The demodulation frequency f_{dem} is chosen so that the center frequency of the received RF signal efficiently becomes zero, which due to frequency-dependent attenuation lies a bit below the pulse transmit frequency f_0.

2) Reduce to lateral map: In general, a 2-D Fourier transform must be calculated in a region near the image focus. Due to the separability of the Fourier transform this can be done first radially and then laterally. Radially the Fourier transform of the received IQ-data can be expressed as:

$$X_{IQ}(f) = \int x_{IQ}(t)\ e^{-j2\pi ft} dt, \tag{3}$$

where x_{IQ} is the complex demodulated signal. However, as we are only interested in the Fourier coefficients at the demodulation frequency, i.e. for $f = 0$ Hz in (3), the integral is reduced to a simple sum of radial samples that can be performed efficiently. This procedure is basically the same as bandpass filtering the RF-signal around the demodulation frequency.

3) Estimate lateral power spectrum: After obtaining the radial Fourier coefficients, the lateral power spectrum is estimated using a discrete Fourier transform. The resulting spectrum will then correspond to the convolution of the transmit and receive aperture functions. A smooth window function such as the Hamming window should be used to reduce variance and sidelobe levels in the estimated power spectrum.

4) Temporal and spatial averaging: To decrease the variance in the spectrum estimates and get a smoother spectrum display, averaging of the lateral power spectrum is done both spatially and between image frames.

5) Log-compress and display: To decrease the high dynamic range of the received signal, log-compression of the lateral power spectrum is done prior visualization. A positive side-effect of the compression is that it also makes the two-way (triangular shape) of the spectrum more similar to a square.

6) Visualization: The lateral power spectrum is visualized as a histogram on screen. The spectrum is mirrored so that the received signal spectrum corresponds to the active part of the transducer aperture.

IV. Results

Using a tissue-mimicking phantom, image data was obtained for 25, 50, 75, and 100 percent effective apertures by masking increasing parts of the aperture in a controlled manner. Further, cardiac imaging examples were acquired to demonstrate the potential usefulness *in vivo*. Data acquisition parameters for all data recordings are given in Table I.

In Fig. 4, a histogram visualization of the lateral power spectrum is shown, calculated using the procedure described in Sec. III. The abscissa has been scaled according to the one-way aperture dimensions. Observe how the lateral spectrum bandwidth closely corresponds to the width of the effective aperture used in each of the cases.

In Fig. 5, two examples of the real-time algorithm are shown, running on a GE Healthcare Vivid 7 ultrasound scanner

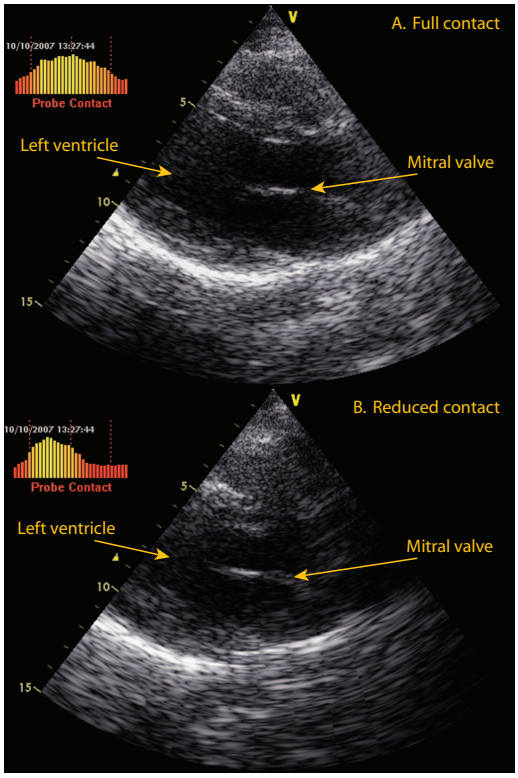

Fig. 5. *In vivo* cardiac imaging examples of the real-time *ProbeContact* application running on a GE Healthcare Vivid 7 scanner (GE Vingmed, Horten, Norway). The histogram display in the upper left corner correctly indicate the different degree of acoustic contact, and also which part of the aperture that is obstructed.

(GE Vingmed, Horten, Norway). Two parasternal imaging views of a healthy heart are shown, where (A) a good acoustic contact is provided, and (B) a reduced acoustic contact is present due to the obstruction caused by the human sternum. As can be seen, in the latter case the lateral resolution has been compromised. Observe that the histogram visualization in the upper left corner of (B) indicate that the right-hand side of the imaging aperture is lacking contact, and therefore that a more suitable probe position should be sought.

V. Discussion

The proposed algorithm is currently limited to the estimation of the two-way aperture function. This two-way func-

TABLE I
Relevant acquisition parameters

Acquisition parameter	Value
Probe	GE M3S
Probe type	1.5D Phased array
Pulse center frequency, f_0	2.5 MHz
No. of pulse periods, N_{pulse}	1.5
F-number	4.0
Image sector width	75 deg
No. of lateral samples	160
Parallel receive beams	none
Transmit / receive apodization	Rectangular

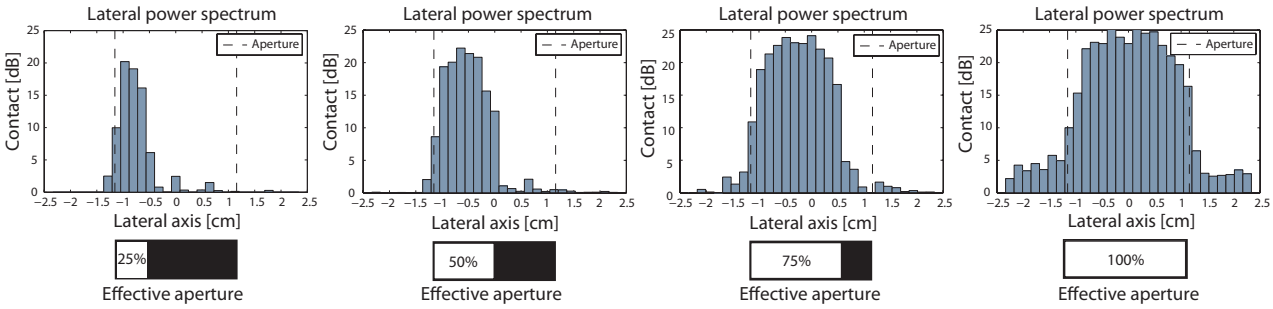

Fig. 4. Tissue mimicking phantom examples. The two-way lateral spectrum calculated as in Sec. III for apertures with an acoustic contact of 25, 50, 75, and 100 percent. The dotted vertical lines indicate the theoretical aperture limits, and the abscissa has been scaled according to the one-way aperture dimensions.

tion corresponds to the actual aperture function in situations when the aperture is obstructed uniformly on one side. The identification situations where the aperture is obstructed non-uniformly to form separate non-overlapping contact regions is more complicated, since the resulting lateral spectrum will then be related to the actual aperture function in a less intuitive way. An alternative could be to approach an estimate of the one-way aperture by decreasing the transmit aperture towards emitting a broad unfocused wave. This would lead to a lateral spectrum that is approximately bandlimited by the receive aperture. The approach is however not suitable for imaging and would require a separate scan sequence in between regular image acquisitions.

Harmonic imaging is used extensively in cardiac imaging [6]. The Fraunhofer relation is then no longer valid on transmit. However, one can in this case approximate the transmit beam profile in focus as the autoconvolution of the transmit aperture. For rectangular apodization functions, the received lateral spectrum will approach a bell-like shape. As a one-sided uniform obstruction of the aperture still infer a similar one-sided lateral bandwidth reduction, the method should also work for harmonic imaging. Preliminary *in vitro* and *in vivo* experiments also indicate this to be the case.

Modern scanners utilize parallel receive beamforming (PRB) to increase the frame rate in 2-D and 3-D ultrasound imaging [7]. This technique has a side effect of invalidating the spatial invariance of the image system, and may lead to artifacts in the lateral spectrum. Recently, methods for correcting the spatial invariance artifacts related to PRB has been proposed that trade off beamforming hardware for improved image quality [8]. These methods may also help reduce artifacts in the proposed method.

Reverberations from obstructing structures close to the transducer aperture may also cause problems for the proposed method, as the reverberated signal may be received for the obstructed transducer elements throughout the depth of the image. This issue should be further investigated.

The indicator has currently been implemented for 2-D imaging, but can easily be extended to 3-D, where a 2-D map of the acoustic contact of matrix arrays can be provided. This will increase the dimensionality of the Fourier transform and therefore the computational complexity.

It is believed that the method might be suited for indication of acoustic contact in 2-D and 3-D transthoracic cardiac imaging, where the narrow spacing between a patient's ribs often can lead to a loss in acoustic window and therefore a reduced image quality. A visual indication of acoustic contact can then help the user guide the probe towards an area of good acoustic window. The method may also be useful in transesophageal imaging, where the probe has to be pushed against the esophagus to form good acoustic contact. Both applications should be further investigated.

VI. Conclusion

The acoustic contact or window in phased-array imaging can be estimated directly through spectral analysis of the received signal in real-time. The bandwidth of the lateral spectrum closely corresponded to the effective imaging aperture in phantom recordings for different degrees of acoustic contact, and further indicated the loss in acoustic contact due to the human sternum in real-time cardiac imaging. We believe the method may help ensure good quality images by aiding the examiner towards finding a probe position with a good acoustic window.

References

[1] R. Lerner and R. Waag, "Wave space interpretation of scattered ultrasound," *Ultrasound Med. Biol.*, vol. 14, pp. 97–102, 1988.

[2] F. Kallel, M. Bertrand, and J. Meunier, "Speckle motion artifact under tissue rotation," *IEEE Trans. Ultrason., Ferroelec., Freq. Contr.*, vol. 41, no. 3, pp. 105–122, 1994.

[3] W. Walker and G. Trahey, "The application of k-space in pulse echo ultrasound," *Ultrasonics, Ferroelectrics and Frequency Control, IEEE Transactions on*, vol. 45, no. 3, pp. 541–558, 1998.

[4] J. W. Goodman, *Introduction To Fourier Optics*, 3rd ed. Roberts & Company Publishers, 2004.

[5] J. Jensen, "Field: A program for simulating ultrasound systems," *Medical & Biological Engineering & Computing,*, vol. 34, no. 1, pp. 351–353, 1996.

[6] F. A. Duck, "Nonlinear acoustics in diagnostic ultrasound," *Ultrasound Med Biol*, vol. 28, no. 1, pp. 1–18, 2002.

[7] O. von Ramm, S. Smith, and J. Pavy, H.G., "High-speed ultrasound volumetric imaging system. ii. parallel processing and image display," *Ultrasonics, Ferroelectrics and Frequency Control, IEEE Transactions on*, vol. 38, no. 2, pp. 109–115, 1991.

[8] T. Hergum, T. Bjastad, K. Kristoffersen, and H. Torp, "Parallel beamforming using synthetic transmit beams," *Ultrasonics, Ferroelectrics and Frequency Control, IEEE Transactions on*, vol. 54, no. 2, pp. 271–280, 2007.